*J. Phys. Chem. A* **1998,** *102,* 7065−7069

# A Direct Ab Initio Dynamics Study on the Finite Temperature Effects on the Hyperfine Coupling Constant of a Weakly Bonded Complex

**Hiroto Tachikawa***

*Division of Molecular Chemistry, Graduate School of Engineering, Hokkaido University, Sapporo 060-8628, Japan*

*Received: April 3, 1998; In Final Form: June 17, 1998*

Finite temperature effects on the hyperfine coupling constant (HFCC) of a weakly bonded molecular complex have been investigated by a direct ab initio dynamics method. The complex composed of methyl radical and HF molecule, $CH_3$···HF, was chosen as a model of the weakly bonded molecular complex. This complex was recently found as an intermediate in a hydrogen abstraction reaction F + $CH_4$ by both electron spin resonance (ESR) and infrared (IR) spectroscopies at low temperature. The geometry optimization showed that the HF molecule is weakly bound to the carbon atom of $CH_3$, and the H atom of HF molecule coordinates toward the central carbon atom. The complex is stabilized by 2.8 kcal/mol at the UMP4SDQ/6-311G(d,p)//UMP4SDQ/6-311G(d,p) level. The direct ab initio dynamics calculation indicated large temperature dependence of HFCCs that is, [$^{13}$C]HFCC increases with increasing temperature, whereas the H and F atoms in the HF molecule, and the methyl hydrogen are decreased. This large change is due to the fact that the structure of the complex is significantly varied by thermal activation. The electronic state of the complex is discussed on the basis of theoretical results.

## 1. Introduction

Hydrogen atom abstraction reaction has been extensively studied from both theoretical and experimental points of view[1,2] because the reaction plays an important role in combustion process and in atmospheric reactions. Because the hydrogen abstraction reaction

$$\mathrm{A} + \mathrm{H{-}B} \rightarrow [\mathrm{A\cdots H\cdots B}] \text{ (transition state, TS)}$$

$$\mathrm{TS} \rightarrow [\mathrm{A{-}H\cdots B}] \text{ (complex)} \rightarrow \mathrm{A{-}H} + \mathrm{B}$$

generally possesses a large available energy, the complex (or chemical intermediate) formed by the reaction is rapidly decomposed to A−H and B, where A and B are heavy atoms, and H is hydrogen. The matrix isolation technique provides an important information on the reaction intermediate.[3] In particular, electron spin resonance (ESR) and Fourier transform infrared (FT-IR) methods combined with the matrix isolation technique are the best way to investigate the electronic state and structure of the chemical intermediate stabilized in matrix.[3,4]

Recently, Misochko et al.[5] detected an intermediate in the hydrogen abstraction reaction by F atom from $CH_4$ molecule in Ar matrix

$$\mathrm{F} + \mathrm{CH_4} \text{ (reactant)} \rightarrow \mathrm{F\cdots H\cdots CH3} \text{ (transition state, TS)}$$

$$\mathrm{TS} \rightarrow \mathrm{HF\cdots CH_3} \text{ (intermediate)} \rightarrow \mathrm{HF} + \mathrm{CH_3} \text{ (product)}$$

by means of ESR measurement. They observed the hyperfine coupling constant (HFCC) of the intermediate and indicated that the intermediate is composed of $CH_3$ radical and HF molecule (i.e., the complex $H_3C$···HF). They showed that an unpaired electron in the complex is mainly localized on the methyl carbon, but slightly diffused to the H of the HF molecule. This result suggests that the HF molecule is weakly bound to the $CH_3$ by the H bond in which the H coordinates toward the methyl carbon. This feature was assigned by the ab initio MO calculation by Misochko et al.[5] They also showed that the H of HF is very flexible around the $CH_3$ radical. The latter fact strongly suggests that temperature dependency of HFCC is possibly observed experimentally.

Experimental work on the HFCC of the other weakly bonded complexes has been conducted by several workers.[4a,6] From a theoretical point of view, the static properties of weakly bonded complexes such as $H_3C$···$CH_4$ and $H_3C$···HCl have been investigated mainly by ab initio MO calculations.[7] However, information on the dynamics feature (i.e., finite temperature effect) is scarcely known because there is no suitable theoretical treatment of the finite temperature effects of the radical and its complexes. Recently, we have made a theoretical calculation on the temperature effect on the structures and electronic states for the neutral and ionic species of $CCl_4$.[8] The calculations were carried out by using the full dimensional potential energy surface (PES) calculated at the ab initio MO level and the classical trajectory was run on the PES. This procedure is called the direct ab initio dynamics calculation.

In the present study, the temperature dependence of the structure and contact spin density (hyperfine coupling constant, HFCC) for the complex $H_3C$···HF is investigated by means of the direct ab initio dynamics calculation. The main propose of this study is to predict qualitatively the thermal energy effect on HFCC of the weakly bound complex $H_3C$···HF. The present theoretical study may provide a deeper insight into the finite temperature effect on the structure and electronic states of the weakly bonded complex.

## 2. Method of Calculations

**Ab Initio MO Calculation.** The complex composed of $CH_3$ radical with HF molecule was chosen as a model of weakly

---

* Fax: +81 11-706-7897. E-mail: hiroto@eng.hokudai.ac.jp.

S1089-5639(98)01733-2 CCC: $15.00

bonded molecular complex. Geometries for the complex, $CH_3$ radical, and HF molecule were fully optimized at the UHF/6-31G*, UMP2/6-31G(d,p), and UMP4SDQ/6-311G(d,p) levels of theory.[9] Because the state energies of the stable and unstable molecules have been known to be strongly affected by electron correlation and the choice of basis sets, we carefully checked the effects of the basis sets and electron correlation on the calculated results. By considering these effects, HFCC of the complex was calculated by the UMP4SDQ/6-311G(d,p) method at each selected point of the trajectory calculation. In all calculations, the expected values of $\langle S^2 \rangle$ without spin annihilation were $<0.7605$.

**Direct Ab Initio Dynamics Calculation.** In general, the classical trajectory is performed on an analytically fitted potential energy surface as previously carried out by us.[10] However, it is not appropriate to predetermine the reaction surfaces of the present systems because of the large number of degrees of freedom ($3N - 6 = 12$ where $N$ is number of atoms in the system). Therefore, in the present study, we applied the direct ab initio trajectory calculation with all degrees of freedom. The detail of direct dynamics method is described elsewhere.[8,11]

In the direct ab initio dynamics calculation, we used the 6-31G* basis set for the complex throughout. Initial structures of the complex were chosen as the optimized one. The trajectories are calculated at several temperatures defined by

$$T = \frac{1}{3Nk} \langle \sum_{i=1}^{N} m_i \, v_i^2 \rangle$$

where $N$ is number of atoms, $v_i$ and $m_i$ are velocity and mass of $i$-th atom, respectively, and $k$ is the Boltzman constant. The potential energy (total energy) and energy gradient were calculated at each time step. In the calculation of the classical trajectory, we assumed that each atom moves as a classical particle on the 6-31G* multidimensional potential energy surface. The equations of motion for **n** atoms in a molecule are given by

$$\frac{\mathrm{d}\, Q_j}{\mathrm{d}t} = \frac{\partial H}{\partial P_j}$$

$$\frac{\partial\, P_j}{\partial t} = - \frac{\partial H}{\partial Q_j} = - \frac{\partial U}{\partial Q_j}$$

where $j = 1-3\ N$, $H$ is the classical Hamiltonian, $Q_j$ is the Cartesian coordinate of the $j$-th mode, and $P_j$ is the conjugated momentum. These equations were numerically solved by the Runge−Kutta method. No symmetry restriction was applied to the calculation of the gradients in the Runge−Kutta method. The time step size was chosen as 0.10 fs, and a total of 5000 steps was calculated for each simulation. Ten snapshots of the trajectory are sampled at every 50-fs interval and then the HFCC is averaged for each temperature. The drift of the total energy is confirmed to be <0.1% throughout at all steps in the trajectory. The momenta of the center of mass and the angular momenta around the center of mass are also confirmed to retain at the initial value of zero.

## 3. Results

**TABLE 1: Optimized Structures Calculated at the Several Levels of Theory**[a]

| parameter | UHF/6-31G* | UMP2/6-31G** | UMP4SDQ/6-311G** |
|---|---|---|---|
| $r_1$ | 2.3863 | 2.2517 | 2.2516 |
| $r_2$ | 0.9136 | 0.9256 | 0.9152 |
| $r_3$ | 1.0738 | 1.0761 | 1.0831 |
| $\theta_1$ | 0.2 | 0.5 | 0.2 |
| $\theta_2$ | 94.9 | 95.3 | 93.7 |
| ∠HCH | 119.56 | 119.38 | 119.58 |

[a] Bond length and angle are in angstroms and in degrees, respectively.

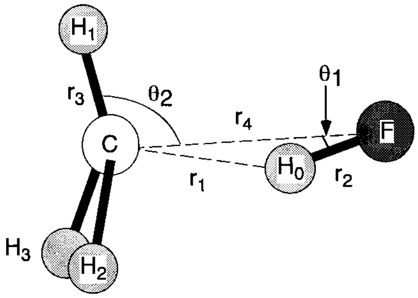

**Figure 1.** Structure and geometrical parameters of $H_3C \cdots HF$ complex.

**A. Ab Initio MO Calculations.** *1. Structure of $H_3C \cdots HF$ Complex.* First, the geometry of the complex was fully optimized at the several levels of theory. The optimized parameters are listed in Table 1. The parameter used for the optimization is schematically illustrated in Figure 1. All calculations gave the similar results on the structure of the complex. Note that the present results of the ab initio calculation are essentially similar to those obtained by Misochko et al.[5] The most sophisticated calculation (UMP4SDQ/6-311G(d,p) level) indicates that the intermolecular distance between $CH_3$ and HF ($r_1$) is 2.2516 Å for the C−H distance. The HF molecule linearly coordinates toward the methyl carbon at the most stable form. The structures of the complex thus obtained are essentially similar to those of the previous work (UMP2/6-31G** level).[5] The H−F distance of the complex is calculated to be 0.9152 Å, which is significantly close to that of free HF molecule (0.9115 Å).

By using the optimized structures, HFCCs are calculated at the MP4SDQ/6-311G(d,p) level. The results are listed in Table 2 together with Mulliken atomic spin densities on the atoms given in parentheses. For comparison, the results of double excitation configuration interaction (CID) and MP2 calculations with aug-cc-pVDZ basis set are given in Table 2. All calculations gave the similar qualitative results. The hydrogen atoms ($H_0$ and H) have negative HFCCs, whereas F and C atoms have positive ones. A simple Mulliken population shows that the unpaired electron is mainly localized on the *p*-orbital of the carbon atom (population on the carbon atom is calculated to be 1.130), although the electron is slightly diffused to the HF molecule. The HFCCs on H and F atoms of the HF molecule are large enough to observe ESR signal of spin on HF molecule. The result of MP4SDQ/6-311G(d,p)//HF/6-31G* calculation is in good agreement with that of MP4SDQ/6-311G(d,p)//MP4SDQ/6-311G(d,p) level. Hence, we calculate the HFCC including the finite temperature effects at the MP4SDQ/6-311G(d,p)//HF/6-31G* level of theory.

*2. Vibrational Frequencies of the Complex $H_3C \cdots HF$.* Table 3 shows the harmonic vibrational frequencies of the complex calculated at the HF/6-31G* level. The vibrational mode of highest frequency, 4298 $cm^{-1}$, corresponds to the H−F stretching mode in the complex. This value is slightly smaller than that of free HF molecule (4357 $cm^{-1}$). This result means that HF bond becomes weaker in the complex formation. The bending mode of $C \cdots H \cdots F$ was calculated to be 111 $cm^{-1}$, suggesting that large amplitude motion of HF may occur around the $CH_3$ radical by thermal energy. In addition, intermolecular stretching mode between the $CH_3$ radical and the HF molecule

**TABLE 2: Hyperfine Coupling Constants (in gauss) on Each Atom Calculated at the Several Levels of Theory (Mulliken Atomic Spin Populations are Given in Parentheses)**

| theory level | $H_0$ | F | C | H |
|---|---|---|---|---|
| CID/aug-cc-pVDZ //UMP4SDQ/6-311G(d,p) | −2.3 (−0.004) | 12.5 (0.004) | 58.4 (1.22) | −24.6 (−0.072) |
| MP2/aug-cc-pVDZ //UMP4SDQ/6-311G(d,p) | −1.31 (−0.004) | 12.8 (0.004) | 55.6 (1.21) | −23.2(−0.069) |
| UMP4SDQ/6-311G(d,p) //UHF/6-31G* | −2.9 (0.013) | 8.6 (0.009) | 25.4 (1.14) | −24.8 (−0.053) |
| UMP4SDQ/6-311G(d,p) //UMP2/6-31G** | −2.9 (0.012) | 16.0 (0.014) | 24.6 (1.15) | −24.3 (−0.053) |
| UMP4SDQ/6-311G(d,p) //UMP4SDQ/6-311G(d,p) | −4.2 (0.012) | 12.7 (0.013) | 23.8 (1.13) | −24.8 (−0.053) |

**TABLE 3: Harmonic Vibrational Frequencies (in $cm^{-1}$) of $H_3C\cdots HF$ Complex Calculated at the UHF/6-31G* Level**

| mode | assignment | sym. | frequency[a] | expl[b] |
|---|---|---|---|---|
| 1 | (H−F) str. | $A_1$ | 4298 (3954) | 3764 |
| 2 | (C−H) asym. str. | $E$ | 3452 (3176) | |
| 3 | (C−H) sym. str. | $A_1$ | 3277 (3015) | |
| 4 | ($CH_2$) sci. | $E$ | 1543 (1420) | |
| 5 | ($CH_3$) bend | $A_1$ | 631 (581) | 664 |
| 6 | ($F-H_0-C$) bent | $E$ | 325 (299) | |
| 7 | ($CH_3$) rock | $E$ | 111 (102) | |
| 8 | [($H_3C$)−(HF)] str. | $A_1$ | 110 (101) | |

[a] Scaled vibrational frequencies (scaling factor is 0.92) are given in parentheses. [b] Experimental values in Ar matrix cited from ref 3b.

is calculated to be 110 $cm^{-1}$, which is significantly small due to the weak interaction. This result implies that the structure of the complex may be easily deformed by the thermal activation. Furthermore, the low frequencies for intermolecular stretching and F−H−C bending modes indicate that the classical trajectory would provide a reasonable structure activated by thermal activation. Therefore, we treated the dynamics of $H_3C\cdots HF$ complex by using the direct ab initio dynamics calculation.

**B. Direct Ab Initio Dynamics Calculations.** *1. Sample Trajectory.* The result of the trajectory calculation is given in Figure 2. In this section, we will discuss the dynamics by using the result obtained for 90 K as a sample trajectory. The potential energy (PE) is gradually fluctuated as a function of simulation time. As shown in Figure 2A, PE is composed of at least two frequency parts: high- and low-frequency parts. The high- and low-frequency parts are assigned to be the H−F stretching mode and ($H_3C$)$\cdots$(HF) intermolecular stretching mode, respectively. Hence, PE is gradually varied by the coupling of two modes. The intermolecular distance ($r_1$) is widely varied from 2.30 to 2.62 Å (Figure 2B), suggesting that the HF molecule is very weakly bound with the methyl radical. The fine structure observed on the $r_1$-curve originates from the H−F stretching mode.

The change of bending angles is plotted in Figure 2C. The bending mode of $\nu_2$ umbrella of $CH_3$ radical is periodically vibrated around 120° ($\angle H_2-C-H_3$). The angles of $C-F-H_0$ ($\theta_1$) and $F-C-H_1$ ($\theta_2$) are varied by 0−18° and 68−118°, respectively. The large change of the latter two angles suggests that the position of HF molecule from the methyl radical is largely affected by the thermal activation. In addition, the large variation of $\theta_2$ indicates that the $C_3$ axis of $CH_3$, which directs toward the F atom of HF molecule at 0 K, is largely fluctuated at 90 K.

*2. Time Dependence of Hyperfine Coupling Constant (HFCC).* To elucidate the finite temperature effects on the structure and HFCCs of the complex, the direct ab initio dynamics calculation is performed at each temperature. Initial geometries of the complex is chosen by the optimized structure.

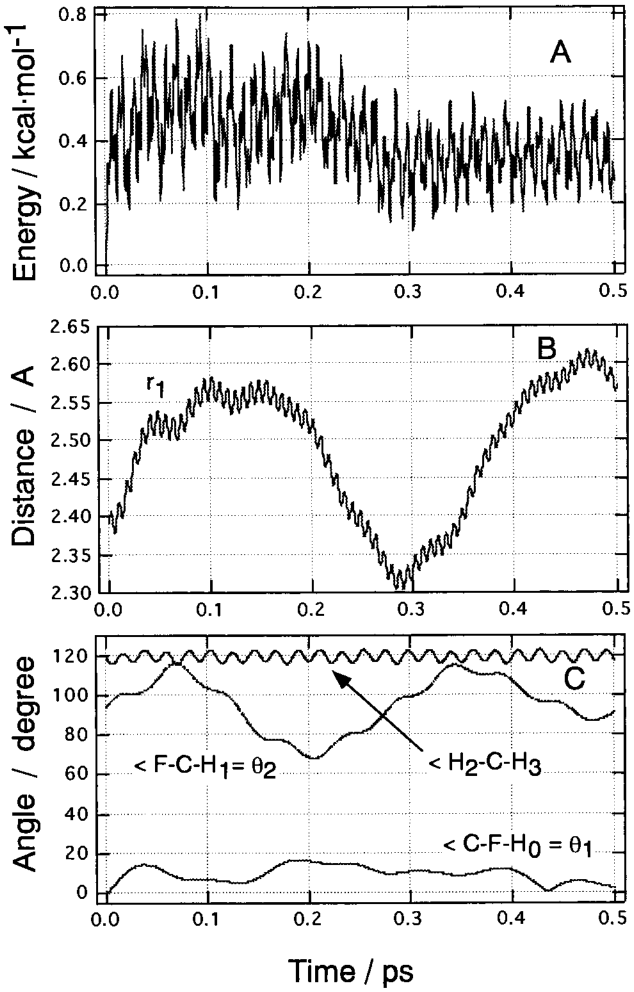

**Figure 2.** A trajectory for the $H_3C\cdots HF$ complex at a constant temperature (90 K) plotted as a function of simulation time: (A) the potential energy of the system; (B) interatomic distance, $r_1$; and (C) the angles, $\angle FCH_1$ ($=\theta_2$), $\angle CFH_0$, and $\angle H_2CH_3$ versus time.

The Fermi contact term, which is linearly proportional to HFCC, is plotted in Figure 3 as a function of simulation time. The Fermi contact terms for $H_0$ and F atoms calculated at only two temperatures (30 and 90 K) are given. As clearly shown in this figure, the Fermi contact terms for both atoms fluctuated largely as a function time. The fluctuation becomes larger at higher temperature, suggesting that the temperature strongly affects the HFCC of the HF molecule. The change for the F atom is larger than that of the H atom.

By comparing Figure 3 with Figure 2B, it is suggested that the HFCC on the HF molecule is larger at the shorter distance of $r_1$ (for example, time = 0.3 ps), meaning that the HFCC is strongly dependent on the distance between the HF molecule and carbon atom. In the case of the complex, the $r_1$ direction

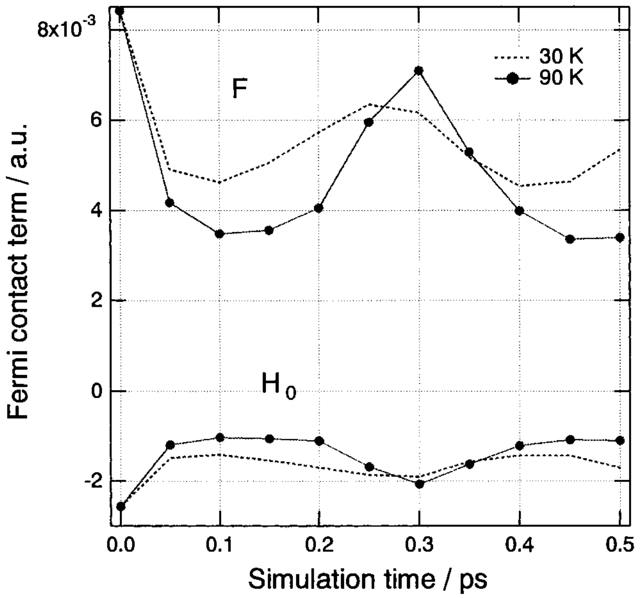

**Figure 3.** Fermi contact terms (in a.u.) calculated as a function of simulation time. The calculations are carried out at constant temperature condition (30 and 90 K).

is one of the large amplitude motions (corresponding to $[(H_3C)-(HF)]_{str}$ mode). Therefore, the HFCC is affected by the thermal activation.

*3. Temperature Dependence of Hyperfine Coupling Constant (HFCC).* As a summary of the trajectory calculations, HFCCs on all atoms calculated as a function of temperature are listed in Table 4. The HFCCs are calculated at the MP4SDQ/6-311G-(d,p) level at each temperature. As clearly seen in Table 4, the absolute values of HFCC of $H_0$ and $H_{1-3}$ atoms decreases with increasing temperature, indicating that the contact spin densities on both H atoms are decreased as a function of temperature. The feature for the F atom shows the similar tendency. On the other hand, the HFCC of the C atom becomes larger at high temperature. The structural flexibility of the complex causes the large temperature dependence of HFCCs of the complex.

## 4. Discussion

**A. Temperature Dependence of the Hyperfine Coupling Constant.** In the present study, we predicted that the HFCCs of the $H_3C\cdots HF$ complex are significantly affected by thermal energy. This result is due to the fact that the HF molecule is weakly bonded to the methyl radical and the structure of the complex is very floppy. In addition, the umbrella motion of $CH_3$ is significantly flexible. Hence, the HFCCs are varied by thermal activation. The present calculations qualitatively indicated that absolute values of the HFCC for the H atoms ($H_0$ and $H_{1-3}$ atoms), which is linearly proportional to the contact spin density on atom, decrease with increasing temperature. The HFCC for F atom is also decreased, whereas that for the C atom slightly increases. The decrease of the contact spin densities (or HFCCs) on HF moiety is due to the fact that the averaged intermolecular distance between $CH_3$ radical and HF molecule, $\langle r_1 \rangle$, is elongated by the thermal activation. The potential energy curve is very flat and loose for $r_1$ direction. This reason accounts for the strong temperature dependence of HFCCs.

The present calculation indicated that the absolute value of HFCC for the H of methyl radical decreases with increasing temperature ($|a_H(0\ K)| = 24.7$ G and $|a_H(90\ K)| = 23.8$ G, where $|a_H(T)|$ means the magnitude of HFCC at $T$ K). This difference is large enough to observe the change of HFCC by ESR spectrometer. The decrease calculated for the H is due to the fact that the $v_2$ umbrella bending mode of $CH_3$ is activated by the thermal energy. This mode activation also causes the increase of HFCC of the C atom. This feature is very similar to that of free methyl radical and consistent with the previous study obtained for the organic free radicals.[12,13]

**B. Comparison with Previous Studies.** In 1995, Misochko et al.[5] observed the complex $H_3C\cdots HF$ formed by a H abstraction reaction F + $CH_4$. First, photolysis of $F_2$ yielded mostly $CH_3$ radical at 14 K. After warming of the photolyzed sample to 21 K, two new radicals form in addition to $CH_3$ radical. One of them is $H_3C\cdots HF$ complex formed by the recombination in cage reaction. The other one is $CH_2F$ radical formed in a secondary reaction of thermal F atoms with the product of cage reaction. The HFCCs for the H atoms of the complex measured by them are −2 G for HF H and −23 G for methyl H in the Ar matrix. The HFCCs for the H atoms calculated in the present work are in excellently agreement with their experiment: $H_0 = -2.87$ G (theory) and −2 G (exptl), H = −24.7 G (theory) and −23 G (exptl). This result implies that the level of theory employed here is enough to estimate HFCC of the complex. As far as we know, there is no experimental data of the temperature dependence of HFCCs of the complex $H_3C\cdots HF$. To confirm the present prediction, experimental work to measure the HFCCs of the complex as a function of temperature is required for a future work.

The IR frequency of the $CH_3\cdots HF$ complex stabilized in the Ar matrix was measured by Jacox.[3b] The experimental values are given in Table 3. Detailed isotropic substitution studies resulted in the assignment of 664 cm$^{-1}$ absorption to the out-of-plane $CH_3$ deformation fundamental to $CH_3\cdots HF$, to 3764 cm$^{-1}$ absorption for the H−F stretching fundamental of $CH_3\cdots HF$. The photolysis of Ar:$CH_4$:$F_2$ samples confirmed the assignment of 1003 cm$^{-1}$ peak to $CH_3F\cdots HF$ complex.[15] In the present study, the H−F stretching and $CH_3$ bending modes are calculated to be 3954 and 581 cm$^{-1}$ (scaled values), respectively, which is in reasonably good agreement with the experiments (3764 and 664 cm$^{-1}$), although the calculated values are slightly shifted from the experimental values. In general, the high- and low-frequency modes of molecule are red- and blue-shifted in the condensed phase, respectively. Therefore, the present calculation of $H_3C\cdots HF$ is consistent with the experiments.

**C. Concluding Remarks.** We have introduced several approximations to calculate the potential energy and to treat the reaction dynamics. First, we assumed that the atom behaves as a classical particle in the multidimensional potential energy

**TABLE 4: Temperature (*T*) Dependence of Fermi Contact Terms (in a.u) [Hyperfine Coupling Constants ($a_H(T)$ in gauss) are Given in Parentheses]**

| *T*, K | $H_0$ | F | C | H |
|---|---|---|---|---|
| 0.0 | −0.00180 (−2.87) | 0.0057 (8.60) | 0.0634 (23.80) | −0.0155 (−24.70) |
| 30 | −0.00161 (−2.57) | 0.0054 (8.15) | 0.0589 (23.60) | −0.0154 (−25.56) |
| 60 | −0.00145 (−2.32) | 0.0048 (7.24) | 0.0598 (23.96) | −0.0153 (−24.40) |
| 90 | −0.00132 (−2.11) | 0.0044 (6.64) | 0.0625 (25.00) | −0.0149 (−23.77) |

surface. The quantum effect was not considered in the present calculations. Especially, the zero point vibrational energy (ZPE) of the system was neglected in the trajectory calculation. This may cause slight change of the HFCC at very low temperature and the dynamics of the complex. The HFCCs at 0 K would be underestimated. To obtain deeper insight on HFCCs at near 0 K, the inclusion of ZPE (i.e., quantum mechanical treatment) on multidimensional potential energy surface would be required.

Second, we assumed HF/6-31G* multidimensional potential energy surface in the trajectory calculations throughout. By using the geometry generated by HF/6-31G* dynamics calculation, the HFCC is calculated at the MP4SDQ/6-311G(d,p) level. The dynamics calculation with more accurate wave function may provide deeper insight in the detailed dynamics. Despite the several assumptions introduced here, the results enable us to obtain valuable information on the finite temperature effect on the spin density on the weakly bonded complex.

In the present study, we neglected matrix effect on the dynamics. However, it may be possible to simulate such a process in Ar matrix using the following procedure. Consider the dynamics of $CH_3\cdots HF$ complex in the Ar cluster. The interactions between Ar atoms can be well approximated using the Lennard−Jones (L−J) potential function. Also, the interaction between atoms in the complex and surrounding Ar atoms may be approximated with the L−J potential. Only for the complex would the ab initio MO method be employed. Such a theoretical simulation is currently being undertaken in our laboratory.

**Acknowledgment.** The author is indebted to the Computer Center at the Institute for Molecular Science (IMS) for the use of the computing facilities. The author acknowledge partial support from a Grant-in-Aid from the Ministry of Education, Science, Sports and Culture of Japan.

## References and Notes

(1) Truhlar, D. G.; Isaacson, A. D.,; Garrett, B. C. In *Theory of Chemical Reaction Dynamics*; Baer, M., Ed; CRC: Boca Raton, FL, 1985; Vol. 4, and reference therein.

(2) Miller, W. H. In *Tunneling*; Jortner, J.; Pullman, B., Eds.; D. Reidel: Boston, 1986, and reference therein.

(3) (a) Jacox, M. E. *Rev. Chem. Intermed*. **1985**, *6*, 77; (b) Jacox, M. E. *Chem. Phys*. **1979**, *42*, 133.

(4) (a) Lund, A.; Shiotani, M. In *Radical Ionic Systems*; Lund, A., Ed.; Kluwer: Dordrecht, 1991; (b) Lunell, S.; Eriksson, L. A.; Fangstrom, T.; Maruani, J.; Sjoqvist, L.; Lund, A. *Chem. Phys*. **1993**, *171*, 119; (c) Huang, M.-B.; Lunell, S.; Karlsson, K. *Chem. Phys. Lett.* **1990**, *171*, 265; (d) Itagaki, Y.; Shiotani, M.; Tachikawa, H. *Acta. Chim. Scand*. **1997**, *51*, 220.

(5) Misochko, E. Y.; Benderskii, V. A.; Goldschleger, A. U.; Akimov, A. V.; Schestakov, A. F. *J. Am. Chem. Soc.* **1995**, *117*, 11997.

(6) *Chemistry and Physics of Matrix-Isolated Species*; Andrews, L., Moskovist, M., Eds.; Elsevier: Amsterdam, 1989; references therein.

(7) (a) Jursic, B. S. *Chem. Phys. Lett.* **1995**, *244*, 263; (b) Chen, Y.; Tshkuikow-Roux, E.; Rauk, A. *J. Phys. Chem*. **1991**, *95*, 9832.

(8) Tachikawa, H. *J. Phys.Chem. A* **1997**, *101*, 7454.

(9) *Ab initio MO calculation program: Gaussian 94*; Frisch, M. J.; Trucks, G. W.; Schlegel, H. B.; Gill, P. M. W.; Johnson, B. G.; Robb, M. A.; Cheeseman; J. R.; Keith, T.; Petersson, G. A.; Montgomery, J. A.; Raghavachari, K.; Al-Laham, M. A.; Zakrzewski, V. G.; Ortiz, J. V.; Foresman, J. B.; Cioslowski, J.; Stefanov, B. B.; Nanayakkara, A.; Challacombe, M.; Peng, C. Y.; Ayala, P. Y.; Chen, W.; Wong, M. W.; Andres, J. L.; Replogle, E. S.; Gomperts, R.; Martin, R. L.; Fox, D. J.; Binkley, J. S.; Defrees, D. J.; Baker, J.; Stewart, J. P.; Head-Gordon, M.; Gonzalez, C.; Pople, J. A. *Gaussian 94, Revision D.3*; Gaussian, Inc.: Pittsburgh PA, 1995.

(10) (a) Tachikawa, H. *J. Chem. Phys.* **1998**, *108*, 3966; (b) Tachikawa, H.; Ohnishi, K.; Hamabayashi, S.; Yoshida, H. *J. Phys. Chem.* **1997**, *101*, 2229; (c) Tachikawa, H. *J. Phys. Chem.* **1995**, *99*, 225; (d) Abe, M.; Inagaki, Y.; Springsteen, L. L.; Matsumi, Y.; Kawasaki, M.; Tachikawa, H. *J. Phys. Chem.* **1994**, 98, 12641; (e) Tachikawa, H.; Hamabayashi, T.; Yoshida, H. *J. Phys. Chem.* **1995**, *99*, 16630; (f) Tachikawa, H.; Takamura, H.; Yoshida, H. *J. Phys. Chem.* **1994**, *98*, 5298; (g) Tachikawa, H.; Ohtake, A.; Yoshida, H. *J. Phys. Chem.* **1993**, *97*, 11944.

(11) (a) Tachikawa, H. *J. Phys. Chem.* **1996**, *100*, 17090; (b) Tachikawa, H.; Komaguchi, K. *Int. J. Mass Spectrom. Ion Processes* **1997**, *164*, 39.

(12) Straff, R. M.; Desjardins, S. G. *J. Am. Chem. Soc.* **1984**, *106*, 256.

(13) (a) Chipman, D. M. *J. Chem. Phys*. **1983**, *78*, 3112; (b) Staikova, M.; Peyerimhoff, S. D.; Zulicke, L. *J. Mol. Spectrosc.* **1995**, *170*, 356; (c) Barone, V.; Grand, A.; Minichino, C.; Subra, R. *J. Phys. Chem.* **1993**, *97*, 6355; (d) Carmichael, I. *J. Phys. Chem.* **1991**, *95*, 108; (e) Huang, M-B.; Lunell, S. *Chem. Phys*. **1990**, *147*, 85.

(14) Jacox, M. E. *Chem. Phys.* **1981**, *59*, 199.

(15) Andrews, L. *J. Phys. Chem.* **1984**, *88*, 2940.